Angiotensin II induces RAW264.7 macrophage polarization to the M1-type through the connexin 43/NF-κB pathway

LEI WU[1,2*], KAI CHEN[1,3*], JINGJIE XIAO[1,4], JUNZHOU XIN[3], LIANG ZHANG[1,4], XINZHI LI[1,4], LI LI[1,4], JUNQIANG SI[1,4], LI WANG[3] and KETAO MA[1,4]

[1]Key Laboratory of Xinjiang Endemic and Ethnic Diseases, Medicine School of Shihezi University, Shihezi, Xinjiang 832008; [2]Department of Cardiology, Taixing People's Hospital, Taixing, Taizhou, Jiangsu 225400; [3]The 3rd Department of Cardiology, The First Affiliated Hospital of The Medical College, Shihezi University; [4]Department of Physiology, Medicine School of Shihezi University, Shihezi, Xinjiang 832008, P.R. China

Abstract. Angiotensin II (AngII) serves an important inflammatory role in cardiovascular disease; it can induce macrophages to differentiate into the M1-type, produce inflammatory cytokines and resist pathogen invasion, and can cause a certain degree of damage to the body. Previous studies have reported that connexin 43 (Cx43) and NF-κB (p65) are involved in the AngII-induced inflammatory pathways of macrophages; however, the mechanisms underlying the effects of Cx43 and NF-κB (p65) on AngII-induced macrophage polarization have not been determined. Thus, the present study aimed to investigate the effects of Cx43 and NF-κB (p65) on the polarization process of AngII-induced macrophages. The macrophage polarization-related proteins and mRNAs were examined by flow cytometry, western blotting, immunofluorescence, ELISA and reverse transcription-quantitative PCR analyses. RAW264.7 macrophages were treated with AngII to simulate chronic inflammation and it was subsequently found that AngII promoted RAW 264.7 macrophage polarization towards the M1-type by such effects as the release of inducible nitric oxide synthase (iNOS), tumour necrosis factor (TNF)-α, IL-1β, the secretion of IL-6, and the expression of M1-type indicators, such as CD86. Simultaneously, compared with the control group, the protein expression levels of Cx43 and phosphorylated (p)-p65 were significantly increased following AngII treatment. The M1-related phenotypic indicators, iNOS, TNF-α, IL-1β, IL-6 and CD86, were inhibited by the NF-κB (p65) signalling pathway inhibitor BAY117082. Similarly, the Cx43 inhibitors, Gap26 and Gap19, also inhibited the expression of M1-related factors, and the protein expression levels of p-p65 in the Gap26/Gap19 groups were significantly decreased compared with the AngII group. Altogether, these findings suggested that AngII may induce the polarization of RAW264.7 macrophages to the M1-type through the Cx43/NF-κB (p65) signalling pathway.

Introduction

Atherosclerosis is the most common cause of ischaemic heart disease and stroke; it is closely associated with the occurrence of acute cardiovascular events, which have a huge impact on human life and health, accounting for 20% of total mortalities worldwide (1). It is widely known that during the early stages of atherosclerosis, monocytes enter the endothelial layer and differentiate into macrophages under the action of adhesion molecules and cytokines (2-4). For example, in one previous study, autopsies of patients with atherosclerosis discovered the accumulation of a large number of macrophages, lymphocytes and foam cells in the coronary artery plaques (2). Macrophages are mainly divided into two different subtypes: M1-type macrophages are mainly found in unstable plaques, whereas M2-type macrophages are predominantly found in stable plaque tissue (5,6). During the development of the disease, various external factors affect macrophages, and depending on the M1/M2 polarization status, the corresponding inflammatory process is highly different (5,7). Binesh *et al* (7) found that pro-inflammatory macrophages (M1-type) were expressed in atherogenic diet-induced aorta, while anti-inflammatory macrophages (M2-type) were expressed in diosgenin-treated aorta. Therefore, improving the condition of the disease by regulating the polarization of M1-type macrophages may be one mechanism to control immune regulation in atherosclerosis.

It has previously been reported that angiotensin II (AngII) can induce macrophages to differentiate towards the M1-type,

Correspondence to: Professor Ketao Ma, Key Laboratory of Xinjiang Endemic and Ethnic Diseases, Medicine School of Shihezi University, 59 North Second Road, Shihezi, Xinjiang 832008, P.R. China
E-mail: maketao@hotmail.com

Professor Li Wang, The 3rd Department of Cardiology, The First Affiliated Hospital of The Medical College, Shihezi University, 107 North Second Road, Shihezi, Xinjiang 832008, P.R. China
E-mail: mcmwl@163.com

*Contributed equally

produce inflammatory cytokines and resist pathogen invasion, whilst also causing damage to the body (8). Increased levels of AngII have been demonstrated to induce the secretion of anti-inflammatory cytokines, and activate NF-κB, adhesion molecules, chemokines, growth factors and oxidative stress (9). NF-κB serves a well-known role in the regulation of immune responses and inflammation, and the NF-κB transcription factor family is comprised of crucial regulatory factors for immune development, immune responses, inflammation and cancer (10). A recent study reported that an increase in the mRNA expression levels of AngII-induced pro-inflammatory cytokines, IL-1β and tumour necrosis factor (TNF)-α, could be blocked by inhibiting the NF-κB pathway (11).

Connexins (Cxs) are one of the basic components of gap junction channels and hemichannels, and are composed of six four-span proteins called connecting proteins (12). The two hemichannel connectors from adjacent cells can be gathered together to form a gap junction that crosses the membrane channel, thus promoting cell-cell communication by transferring a ~1-kDa signalling molecule from one cell to the adjacent cell (13). Connective family molecules, such as Cx30, Cx32, Cx37, Cx40 and Cx43, of which Cx43 is the most common, are also widely expressed in immune cells; these proteins make up the gap junction channels and hemichannels involved in a variety of immunomodulation processes (14). It was previously demonstrated that AngII increased the expression levels of Cx43 in the vascular smooth muscle of hidden veins in a dose- and time-dependent manner, whereas the p38 and ERK MAPK inhibitors, SB203580 and PD98059, inhibited this effect (15). In addition, reduced conductivity of Cx43 channels using Gap26 in a lipopolysaccharide (LPS)-induced inflammatory mouse model effectively reduced the adhesion of neutrophils and endothelial cells, significantly reduced residual bacteria in the abdominal cavity of mice, and significantly improved survival in infected mice (16). However, the mechanisms underlying AngII-induced macrophage polarization have not been determined. The present study aimed to investigate whether Cx43 and NF-κB are involved in AngII-induced macrophage polarization processes by studying the effect of Cx43/NF-κB signalling pathways on the polarization of AngII-induced RAW264.7 macrophages to the M1-type.

Materials and methods

Cell culture and experimental grouping. RAW264.7 macrophages were purchased from the Shanghai Institutes for Biological Sciences, Chinese Academy of Sciences. Cells were plated into a culture flask at a density of $3x10^5$/ml, and were cultured in a CO_2 thermostatic incubator at 37˚C and 5% CO_2 in DMEM (Gibco; Thermo Fisher Scientific, Inc.) supplemented with 10% FBS (Gibco; Thermo Fisher Scientific, Inc.). Cells were passaged upon reaching 70-80% confluence.

RAW264.7 macrophages were treated with 10^{-9}, 10^{-8}, 10^{-7}, 10^{-6} and 10^{-5} mol/l AngII (APExBIO Technology LLC) for 0, 3, 6, 12, 24 and 48 h to determine the optimal treatment conditions. RAW264.7 macrophages were cultured and treated in different ways: i) Control group, macrophages cultured in DMEM/FBS without any treatment; ii) AngII group, in which cells were treated with 10^{-6} mol/l AngII (APExBIO Technology LLC) for 12 h at 37˚C (17,18); iii) Gap26 group, in

which cells were pre-treated with 10^{-4} mol/l Gap26 (APExBIO Technology LLC) at 37˚C for 45 min prior to 10^{-6} mol/l AngII treatment for 12 h (19,20); iv) Cx43 inhibitor Gap19 group, in which cells were pre-treated with $2x10^{-4}$ mol/l Gap19 (APExBIO Technology LLC) at 37˚C for 45 min prior to treatment with 10^{-6} mol/l AngII for 12 h (20); v) DMSO group, in which cells were treated with 10^{-6} mol/l DMSO (Beijing Solarbio Science & Technology Co., Ltd.) for 12 h at 37˚C; and vi) NF-κB signaling pathway inhibitor BAY117082 group, in which cells were pre-treated with 10^{-5} mol/l BAY117082 (cat. no. ab141228; Abcam) for 1 h prior to treatment with 10^{-6} mol/l AngII for 12 h (21,22).

Cell viability assay. Cells ($8x10^3$/well) were seeded into a 96-well plate and treated with increasing concentrations (10^{-9}, 10^{-8}, 10^{-7}, 10^{-6} or 10^{-5} mol/l) of AngII for 12 h at 37˚C. Cell viability was subsequently measured using a Cell Counting Kit-8 (CCK-8) assay (Dojindo Molecular Technologies), according to the manufacturer's protocol.

Flow cytometry. The frequency of CD86 (Invitrogen; Thermo Fisher Scientific, Inc.) expression was detected using flow cytometry. The following were used as blocking (4˚C for 15-30 min) reagents: MouseBD Fc Block (BD Biosciences) and BSA (5%; Sigma-Aldrich; Merck KGaA). Before use, the serum preparations were heat inactivated (56˚C for 45 min) and sterile filtered (0.2-μm filter); the negative cells and CD86 were individually labelled as a control to analyze the data. Cells ($1x10^6$/well) were cultured for 24 h, digested with 0.25% trypsin, centrifuged at 603 x g for 5 min at 37˚C and subsequently retained as a pellet; filter paper was used to absorb as much of the liquid left in the tube as possible. Each pellet was resuspended in 1 ml PBS, centrifuged at 603 x g at 37˚C for 5 min and retained as a pellet. The pellets were resuspended in 200 μl PBS in Eppendorf tubes and 2 μl phycoerythrin (PE)-CD86 antibody (1:100, cat. no. 85-12-0862; Invitrogen; Thermo Fisher Scientific, Inc.) was added to each Eppendorf tube and incubated at 37˚C in the dark for 30 min. Subsequently, PBS was added to each tube and cells were centrifuged at 603 x g for 5 min at 37˚C. The supernatant was discarded and the pellets were resuspended in 200 μl PBS and mixed. A formulated fixative Fixation Concentrate (cat. no. 00-5521-00; 1%; BD Biosciences) was added to each tube at room temperature for 20 min prior to incubation with a PE-CD206 antibody (1:100, cat. no. 85-25-2061; Invitrogen; Thermo Fisher Scientific, Inc.) at 37˚C in the dark for 30 min. Subsequently, cells were resuspended in 1 ml 1X permeabilization reagent (cat. no. 00-8333-56; BD Biosciences) for 30 min at 25˚C and centrifuged at 603 x g for 5 min at 37˚C. The supernatant was discarded and filter paper was used to absorb the liquid left in the tube. Following the suspension of cell pellets in 200 μl PBS, analysis of CD206 and CD86 expression levels was performed using flow cytometry (FACSort; BD Biosciencnes) with BD CellQuest Prosoftware (version 2.0, system OS2; Becton, Dickinson and Company). To ensure the accuracy of the experimental results, all samples were analysed within 3 h to avoid fluorescence changes, which could affect the experimental results. The number of detected cells per tube was 10,000-20,000.

Western blotting. The protein expression levels of CD86, CD206, inducible nitric oxide synthase (iNOS), Cx43, p65

and phosphorylated (p)-p65 were analysed using western blotting. Total protein was extracted from cells using RIPA lysis buffer (cat. no. R0020; Beijing Solarbio Science and Technology Co., Ltd.). Total protein was quantified using a bicinchoninic acid protein assay kit and equal quantities of protein (15 μg/lane) were separated by SDS-PAGE (Beijing Solarbio Science & Technology Co., Ltd.) on 10% gels. The separated proteins were subsequently transferred onto a PVDF membrane (EMD Millipore) and blocked with 5% skim milk in TBS-0.2% Tween-20 (TBST; Sangon Biotech, Co., Ltd.) for 2 h at room temperature. The membranes were incubated with the following primary mouse and rabbit antibodies at 4°C overnight: Anti-CD86 (1:1,000; cat. no. ab53004; Abcam), anti-Cx43 (1:1,000; cat. no. ab11370; Abcam), anti-p65 (1:1,000; cat. no. ab16502; Abcam), anti-p-p65 (1:1,000; cat. no. ab86299; Abcam), anti-iNOS (1:500; cat. no. ab15323; Abcam), anti-CD206 (1:500; cat. no. ab64693; Abcam) and anti-β-actin (1:1,000; cat. no. TA-09; Beijing Fir Jinqiao Biotechnology Co., Ltd.). Following primary antibody incubation, the membrane was washed three times with TBST (10 min/wash) and the secondary antibody (1:10,000; horseradish peroxidase-conjugated goat anti-rabbit; cat. no. ZB-2306; Beijing Zhongshan Jinqiao Biotechnology Co. Ltd.) was subsequently incubated with the PVDF membrane at room temperature for 2 h. The membrane was washed three times with TBST (10 min/wash) and protein bands were visualized on X-ray film using an ECL reagent (GE Healthcare Life Sciences; Thermo Fisher Scientific, Inc.). Protein expression was semi-quantified using ImageJ software (version 1.8.0; National Institutes of Health).

Reverse transcription-quantitative PCR (RT-qPCR). Total RNA was extracted from RAW264.7 macrophages using TRIzol® reagent (Invitrogen; Thermo Fisher Scientific, Inc.). Total RNA (0.5 μg) was RT using a Revert Aid First Strand cDNA Synthesis kit (cat. no. K1622; Thermo Fisher Scientific, Inc.) at 42°C for 60 min and 70°C for 5 min. Total RNA (adjusted to 500 ng, 2.5 μl), Oligo dT PCR primer (50 μM, 1 μl), 5X PrimeScript buffer (4 μl), RiboLock RNase Inhibitor (20 U/μl, 1 μl), 10 mM dNTP Mix (2 μl), RevertAidM-MuLV RT (200 U/μl, 1 μl) and RNase free distilled H_2O (8.5 μl). The synthesized cDNA was amplified by RT-qPCR using SYBR (Applied Biosystems; Thermo Fisher Scientific, Inc.). Each reaction mixture for PCR (total volume 20 μl) consisted of cDNA (adjusted to 500 ng, 1 μl), forward and reverse PCR primers (10 μM, 0.5 μl each), SYBR (10X, 10 μl) and distilled H_2O (8 μl). The themorcycling conditions were as follows: Initital denaturation at 95°C for 2 min for one cycle, followed by 40 cycles of denaturation at 95°C for 5 sec and annealing and extension at 60°C for 31 sec. The relative expression levels of target genes were normalized to rRNA (Applied Biosystems; Thermo Fisher Scientific, Inc.) and were calculated using the $2^{-\Delta\Delta Cq}$ method (23). qPCR with SYBR Green detection was subsequently performed using an Eppendorf Mastercycler ep realplex (Eppendorf). The gene primers (Shanghai GenePharma Co., Ltd.) used were as follows: CD86, forward 5'-ACGGAGTCAATGAAGATTTCCT-3', reverse 5'-GATTCGGCTTCTTGTGACATAC-3'; iNOS, forward 5'-GTTTACCATGAGGCTGAAATCC-3' reverse 5'-CCT

CTTGTCTTTGACCCAGTAG-3', TNF-α, forward, 5'-ATG TCTCAGCCTCTTCTCATTC-3', reverse 5'-GCTTGTCAC TCGAATTTTGAGA-3'; IL-1β, forward 5'-TCGCAGCAG CACATCAACAAGAG-3', reverse, 5'-TGCTCATGTCCTCAT CCTGGAAGG-3'; IL-6, forward 5'-CTCCCAACAGACCTG TCTATAC-3', reverse, 5'-CCATTGCACAACTCTTTTCT CA-3'; and β-actin, forward 5'-CACGATGGAGGGGCCGGA CTCATC-3' and reverse 5'-TAAAGACCTCTATGCCAACAC AGT-3'.

Immunofluorescence. A total of 3x10⁵/ml RAW264.7 macrophages were seeded into 6-well plates at 37°C for 2-3 days with sterile coverslips to make cell slides. Then, slides were washed with PBS (Beijing Solarbio Science & Technology Co., Ltd.) 2-3 times and then fixed with 4% paraformaldehyde for 10-20 min at room temperature. The fixative was washed off three times with PBS (2-3 min/wash). Slides were permeabilized with 0.2% Triton X-100 for 5 min at room temperature, washed three times with PBS for 2-3 min each time and subsequently blocked with 5% BSA (Sigma-Aldrich; Merck KGaA) blocking solution at 37°C for 30 min. Sections were then probed with various primary antibodies [anti-Cx43 polyclonal antibody (1:100; cat. no. ab11370; Abcam), anti-CD86 polyclonal antibody (1:100; cat. no. ab53004; Abcam) and anti-iNOS polyclonal antibody (1:100; cat. no. ab15323; Abcam)], whilst as a negative control, samples were incubated overnight at 4°C with the primary antibody and rewarmed to 37°C for 30 min before the primary antibody was discarded. Samples were washed three times with PBS (3 min/wash) prior to incubation with the fluorescent secondary antibody (1:50; Goat anti-rabbit secondary antibodies; cat. no. ZDR-5209; Beijing Zhongshan Jinqiao Biotechnology Co., Ltd.) at 37°C for 1 h. Following the incubation, the secondary antibody solution was discarded and samples were washed three times with PBS (5 min/wash). Slides were subsequently incubated with propidium iodide (1:1,000; Beijing Solarbio Science & Technology Co., Ltd.) in the dark at room temperature for ~1 min prior to being washed three times with PBS (5 min/wash). An anti-fluorescence attenuating sealer was then added to the slides and stained slides were observed using a Zeiss LSM 510 META laser confocal microscope (magnification, x630; Carl Zeiss AG).

ELISA. The levels of TNF-α, IL-1β and IL-6 in RAW264.7 macrophages (1x10⁶/well) supernatant (Repeated freeze-thaw and high-speed centrifugation (603 x g at 4°C for 5 min) to obtain cell supernatant) were analysed using ELISA kits (TNF-α, cat. no. PMTA00B; IL-1β, cat. no. DY401; IL-6, cat. no. PM6000B; R&D Systems, Inc.), according to the manufacturer's protocols. The absorbance was measured at 450 nm. All absorbance values were within the linear range of the standard curve and the final result was expressed in pg/ml.

Statistical analysis. Data are expressed as the mean ± SEM from ≥6 independent experiments. Statistical analyses were performed SPSS 24.0 (IBM Corp.). Statistical differences between >2 groups were assessed using one-way ANOVA followed by Tukey's post hoc test, whereas statistical differences between two groups were determined using unpaired Student's t-test. $P<0.05$ was considered to indicate a statistically significant difference.

Results

AngII can mediate the polarization of RAW264.7 macrophages to the M1-type. To investigate the effect of different concentrations (0, 10^{-9}, 10^{-8}, 10^{-7}, 10^{-6} and 10^{-5} mol/l) of AngII on the cell viability of RAW264.7 macrophages, a CCK-8 assay was used. It was observed that 10^{-6} mol/l AngII had no significant effect on cell viability compared with the control group; therefore, AngII at a concentration of 10^{-6} mol/l was selected for use in further experiments (Fig. 1A). Flow cytometric analysis was used to detect the expression levels of the M1-type macrophage marker CD86 and the M2-type macrophage marker CD206 in RAW264.7 macrophages. The levels of CD86 expression were significantly increased following AngII treatment compared with the control group (Fig. 1C). There were no significant differences observed in the expression levels of the M2 marker CD206 in the AngII group compared with the control group (Fig. 1C). Furthermore, the protein expression levels of CD86 and iNOS at 3, 6, 12, 24 and 48 h were significantly increased in the AngII group compared with the control group (Fig. 1B). Moreover, this trend in protein expression levels of the M1-type macrophage markers CD86 and iNOS occurred in a time-dependent manner; the protein expression levels of CD86 and iNOS peaked following 12 h of AngII treatment. However, the protein expression levels of the M2 macrophage marker CD206 were not significantly increased in the AngII group compared with the control group after 12 and 24 h. Therefore, in the subsequent experiments, a treatment intervention time of 12 h was used (Fig. 1D).

AngII induces M1-type polarization in RAW264.7 macrophages through the NF-κB (p65) signalling pathway. To investigate the role of NF-κB in AngII-induced macrophage polarization, RAW264.7 macrophages were treated with AngII for 12 h. Western blotting analysis observed that p-p65 expression levels in the AngII group were significantly increased compared with the control group, which indicated that the NF-κB (p65) signalling pathway may be activated by AngII (Fig. 2A). Subsequently, the RAW264.7 macrophages were pre-treated with the NF-κB (p65) signalling pathway inhibitor BAY117082 prior to being incubated with AngII for 12 h. Western blotting revealed that the protein expression levels of CD86 and iNOS in the DMSO group were not significantly different compared with the control group (Fig. 2B); however, the expression levels of CD86 and iNOS in the AngII group were significantly increased compared with the control group. Notably, upon treatment with the NF-κB (p65) signalling pathway inhibitor BAY117082, the protein expression levels of CD86 and iNOS in the BAY117082 group were significantly decreased compared with the AngII group (Fig. 2B).

The results of RT-qPCR analysis demonstrated that the mRNA expression levels of the M1-type markers iNOS, TNF-α, IL-1β, IL-6 and CD86 in RAW264.7 macrophages DMSO group were not significantly different compared with the control group (Fig. 2C). The results showed that DMSO had no effect on cell mRNA expression levels. However, the M1-type markers in the AngII group were significantly increased compared with the control group, whereas they were significantly decreased in the BAY117082 group compared

with the AngII group (Fig. 2C). Furthermore, the levels of the M1-type markers TNF-α, IL-1β and IL-6 were analysed in the supernatants obtained from RAW264.7 macrophages using ELISA. The expression levels in the AngII group were significantly increased compared with the control group (Fig. 2D), whereas the expression levels in the BAY117082 group were significantly decreased compared with the AngII group (Fig. 2D).

AngII increases Cx43 protein expression levels in RAW264.7 macrophages. Following the treatment of RAW264.7 macrophages with 10^{-6} mol/l AngII for 3, 6, 12, 24 and 48 h, the increases in the protein expression levels of Cx43 in macrophages were time-dependent, with the protein expression levels reaching their maximum at 12 h (Fig. 3A). The localization of Cx43 in RAW264.7 macrophages was determined using an immunofluorescence assay. The results discovered that Cx43 was expressed in RAW264.7 macrophages; compared with the control group, the protein expression levels of Cx43 in macrophages was consistent with the results obtained from western blotting at different time points (Fig. 3B).

AngII induces the polarization of RAW264.7 macrophages to the M1-type, and polarization markers are inhibited following pre-treatment of macrophages with the Cx43 blockers Gap26 and Gap19. To investigate the role of Cx43 in macrophage polarization, RAW264.7 macrophages were pre-treated with the Cx43 blockers Gap26 and Gap19 for 45 min prior to AngII treatment for 12 h. Western blotting observed that compared with the untreated control group, the protein expression levels of the macrophage M1-type markers, CD86 and iNOS, were significantly increased following 12 h of AngII treatment (Fig. 4A). Notably, CD86 protein expression was significantly decreased in the Gap19 group compared with the AngII group, whereas iNOS protein expression levels were significantly decreased in the Gap26 and Gap19 groups compared with the AngII group (Fig. 4A). The mRNA expression levels of M1-type markers were subsequently investigated using RT-qPCR. The results demonstrated that the mRNA expression levels of iNOS, TNF-α, IL-1β, IL-6 and CD86 in RAW264.7 macrophages were significantly increased following AngII treatment compared with the control group; however, this effect was significantly inhibited by pre-treatment with Gap26/Gap19 (Fig. 4C). The localization of the M1-type markers CD86 and iNOS in RAW264.7 macrophages was analysed using immunofluorescence. The results indicated that CD86 and iNOS were expressed in RAW264.7 macrophages; compared with the control group, the protein expression levels of M1-type markers CD86 and iNOS were consistent with the results revealed with western blotting (Fig. 4B). In addition, the levels of M1-type cytokines TNF-α, IL-1β and IL-6 in the supernatants of RAW264.7 macrophages were detected using ELISA; the levels of TNF-α, IL-1β and IL-6 in the AngII group were significantly increased compared with the control group; however, this increase was significantly prevented following pre-treatment with Gap26/Gap19 (Fig. 4D). These results suggested that AngII may induce RAW264.7 macrophage polarization to the M1-type by upregulating Cx43 expression.
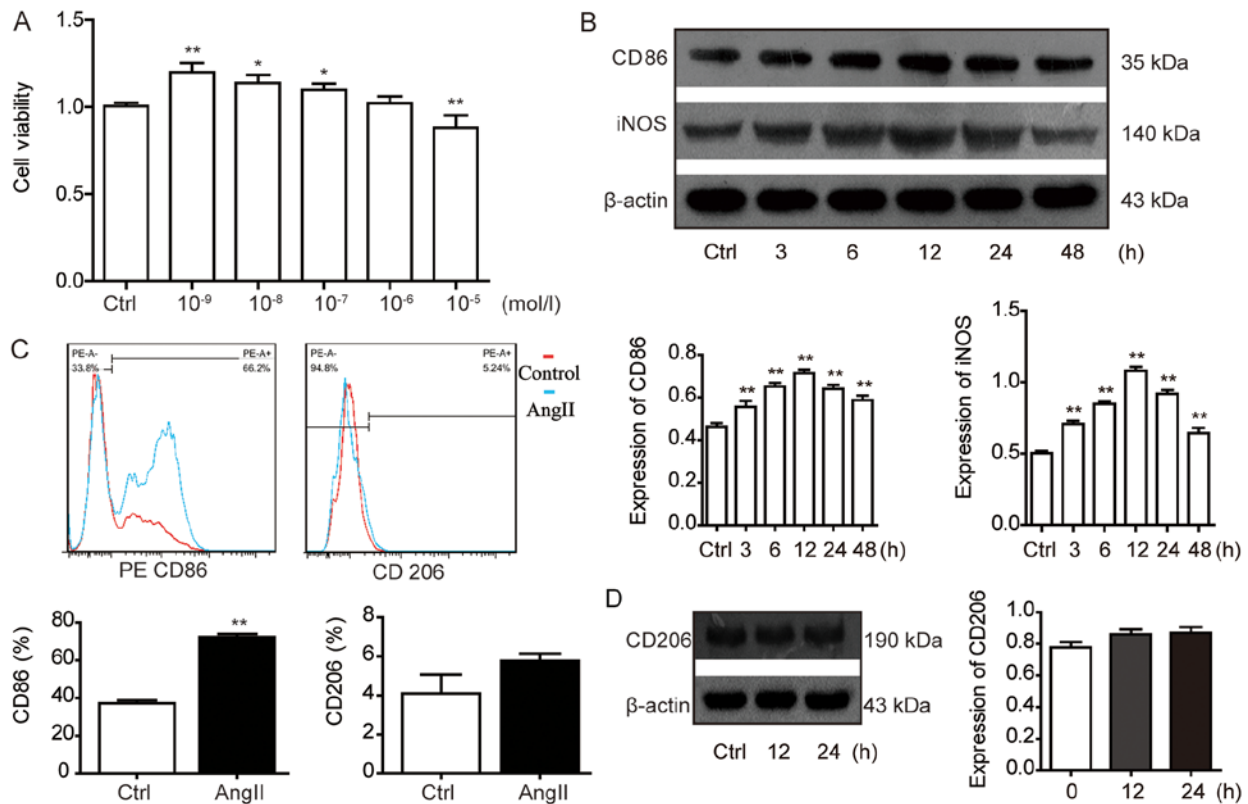
Figure 1. AngII mediates the polarization of RAW264.7 macrophages to the M1-type. (A) Effects of different concentrations of AngII on the cell viability of RAW264.7 macrophages were determined using a Cell-Counting Kit 8 assay. (B) Western blotting was used to detect the expression levels of M1-type macrophage markers, CD86 and iNOS, in RAW264.7 macrophages at different time points. (C) Flow cytometric analysis of the expression levels of CD86 and CD206 in RAW264.7 macrophages and the subsequent semi-quantitative analysis. (D) Western blotting was used to detect the expression levels of the M2-type macrophage marker, CD206, in RAW264.7 macrophages at different time points. Data are presented as the mean ± SEM (n=6). *P<0.05, **P<0.01 vs. Ctrl group. AngII, angiotensin II; Ctrl, control; iNOS, inducible nitric oxide synthase; PE, phycoerythrin.
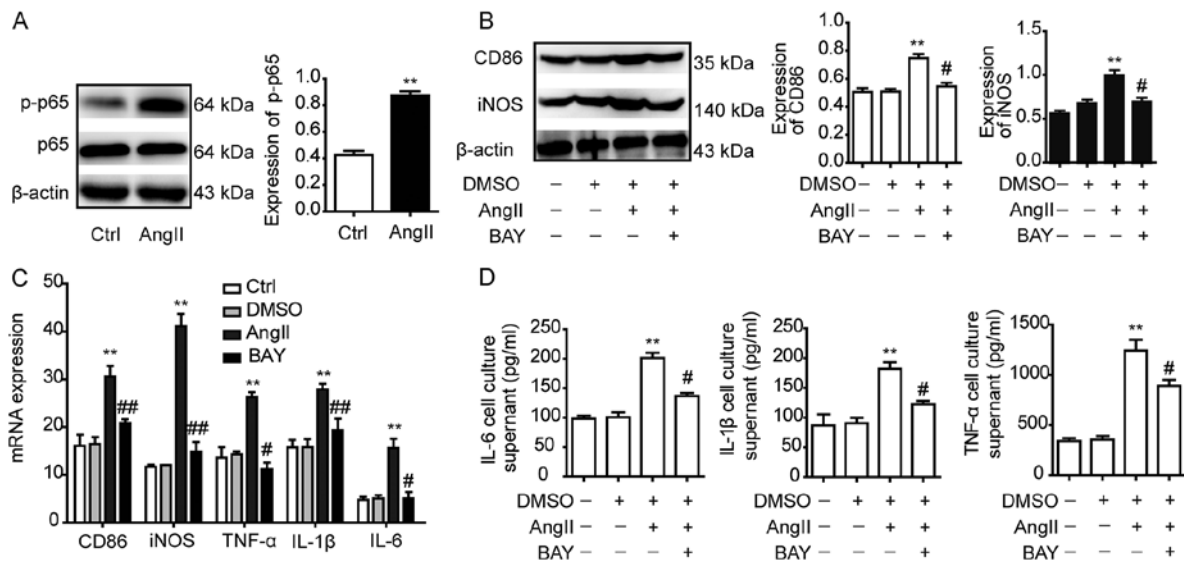

Figure 2. AngII induces polarization of RAW264.7 macrophages to the M1-type through the NF-κB (p65) signalling pathway. Protein expression levels of (A) total p65 and p-p65, and (B) M1-type macrophage markers CD86 and iNOS in RAW264.7 macrophages were detected and semi-quantified using western blotting. (C) Detection of mRNA expression levels of M1-type macrophage markers in RAW264.7 macrophages were detected using reverse transcription-quantitative PCR. (D) Detection of M1-type marker protein levels in the supernatant of RAW264.7 macrophages using ELISA. Data are presented as the mean ± SEM (n=6). **P<0.01 vs. Ctrl group; #P<0.05, ##P<0.01 vs. AngII group. AngII, angiotensin II; BAY, BAY117082; Ctrl, control; iNOS, inducible nitric oxide synthase; p, phosphorylated; TNF, tumour necrosis factor.

AngII activates the NF-κB (p65) signalling pathway by upregulating Cx43 expression. To investigate the relationship between Cx43 and the NF-κB (p65) signalling pathway, RAW264.7 macrophages were pre-treated with the Cx43
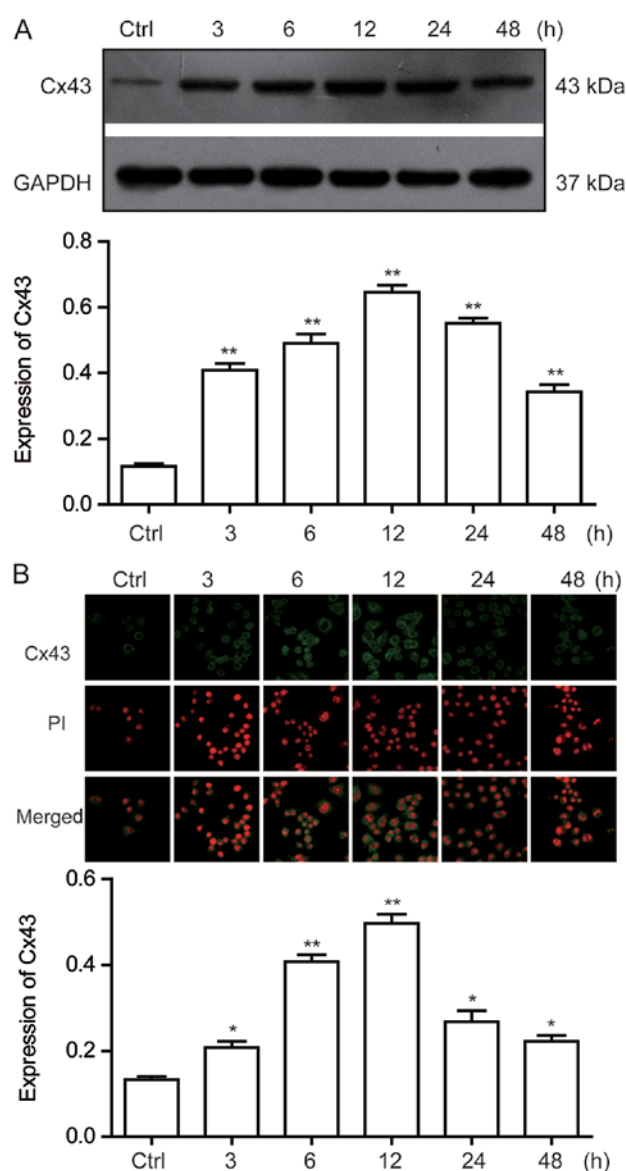
Figure 3. AngII upregulates Cx43 protein expression levels in RAW264.7 macrophages. (A) Western blotting was used to detect the protein expression levels of Cx43 in RAW264.7 macrophages treated with 10^{-6} mol/l AngII at different time points (3, 6, 12, 24 and 48 h). Semi-quantitative analysis of Cx43 protein expression levels in macrophages was subsequently performed. (B) Immunofluorescence assay was used to detect the expression and localization of Cx43 protein in macrophages at different time points (3, 6, 12, 24 and 48 h) following 10^{-6} mol/l AngII treatment and semi-quantitative analysis of Cx43 protein levels in macrophages was conducted. Magnification, x630. Data are presented as the mean ± SEM (n=6). *P<0.05, **P<0.01 vs. Ctrl group. AngII, angiotensin II; Ctrl, control; Cx43, connexin 43; PI, propidium iodide.

blockers Gap26 and Gap19 for 45 min prior to AngII treatment for 12 h. It was revealed that the expression levels of p-p65 in the Gap26 and Gap19 groups were significantly decreased compared with the AngII group, indicating that AngII activates the NF-κB (p65) signalling pathway by upregulating Cx43 expression (Fig. 5).

Discussion

Atherosclerosis is a multifactorial inflammatory disease of the middle to large arterial wall (24), and is one of the leading causes of death in industrialized countries, with incidence rates rapidly increasing in developing countries (25). A large number of macrophages are found to accumulate in atherosclerotic plaques, which subsequently secrete various inflammatory cytokines, further aggravating the accumulation of macrophages in blood vessels, and promoting the continual change and development of atherosclerotic plaques (26). Autopsies of patients with atherosclerosis revealed that a large number of macrophages, lymphocytes and foam cells are found in the coronary plaque, and the ratio of macrophages and lymphocytes is largest in the rupture plaque (25). Macrophages are mainly divided into two different subtypes: M1 and M2, which are predominantly located in unstable plaques and stable plaque tissues, respectively (5,6). It has previously been reported that iNOS, TNF-α, IL-1β, IL-6, IL-12 and CD86 are major markers of M1-type macrophages (27). In addition, AngII was found to stimulate RAW264.7 macrophages to not only promote the production of pro-inflammatory factors, such as TNF-α, IL-1β and IL-6, but also to increase the release of reactive oxygen species (28). Therefore, it was hypothesized that through inhibiting the polarization of macrophages to the M1-type, it may be possible to stabilize vascular plaques and reduce the formation of unstable plaques, which would help identify mechanisms to prevent and treat cardiovascular and cerebrovascular diseases caused by atherosclerosis.

In the present study, RAW264.7 macrophages were used to induce M1-type polarization and it was observed that 10^{-6} mol/l AngII treatment had no significant effect on cell viability. This was consistent with previous findings by Li *et al* (17) and Jiang *et al* (29), who also used this concentration of AngII in their studies. Therefore, this concentration was used in subsequent experiments. It was revealed that CD86 and iNOS expression levels in RAW264.7 macrophages were significantly increased following treatment with AngII, whereas the levels of the M2-type marker CD206 were not affected. The results suggested that AngII may induce M1-type polarization in RAW264.7 macrophages.

It is well known that the NF-κB pathway serves an important role in regulating immune and inflammatory processes, and affects the expression of cytokines that mediate pro-inflammatory responses and inflammation, apoptosis and proliferation (30). The NF-κB (p65) signalling pathway is highly activated in the inflammatory sites with diverse enzymes, which induces the transcription and production of inflammatory cytokines, including IL-1β, IL-6 and TNF-α at the inflammatory site; this pathway is known to serve an important role during the acute phase of the immune response (31). It has previously been reported that treatment with NF-κB (p65) inhibitors significantly reduced mechanically induced inflammatory responses (32). In the present study, to investigate the potential role of the NF-κB (p65) signalling pathway in AngII-induced macrophage M1-type polarization, RAW264.7 macrophages were pre-treated with inhibitors of the NF-κB (p65) signalling pathway. Following treatment with NF-κB (p65) inhibitors, the protein and mRNA expression levels of M1-type macrophage markers were significantly reduced. These results suggested that AngII-induced macrophage polarization to the M1-type may be modulated by the NF-κB (p65) signalling pathway.
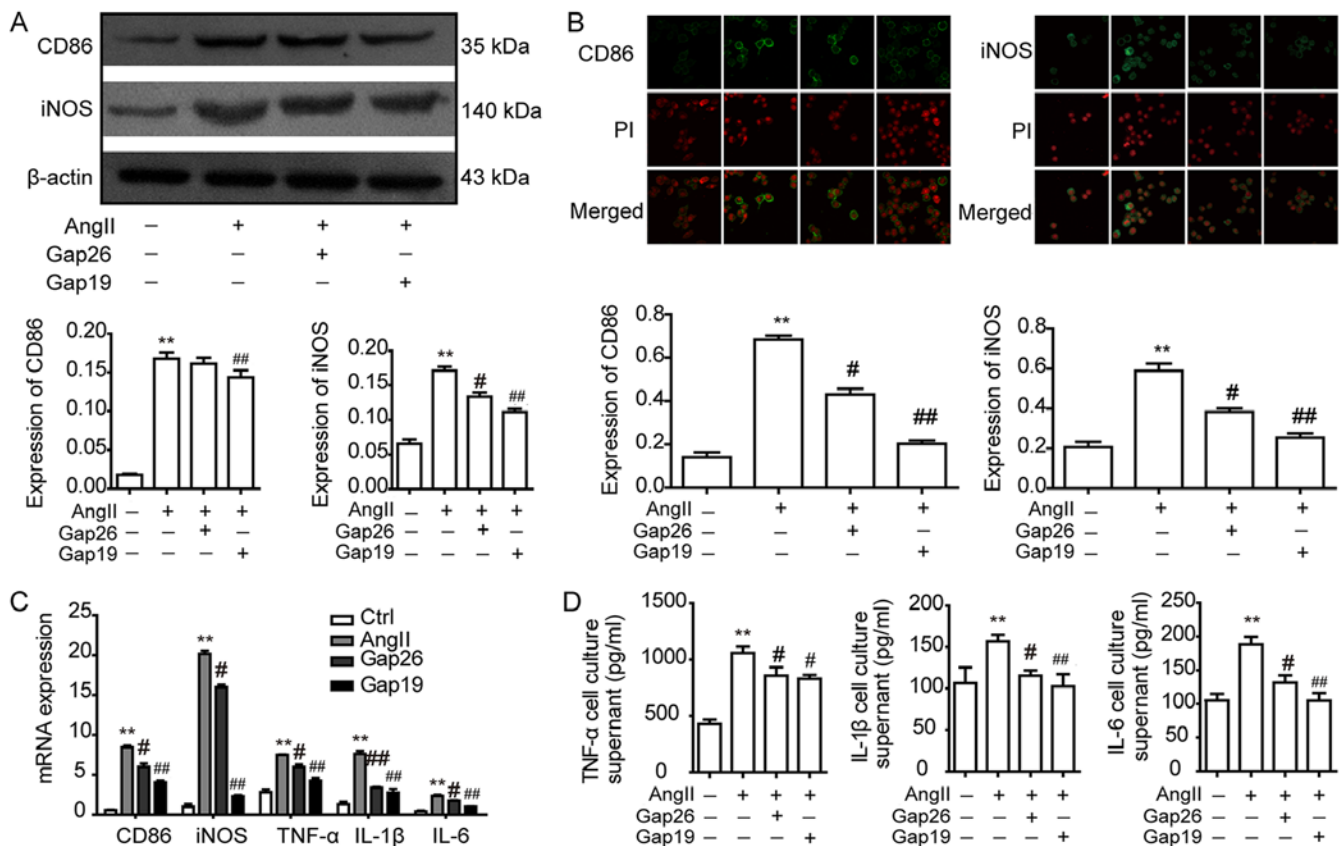
Figure 4. AngII induces RAW264.7 macrophage polarization to the M1-type, and the M1-type polarization markers are inhibited following pre-treatment with the Cx43-specific blockers Gap26 and Gap19. (A) Western blotting was used to analyse and semi-quantify the protein expression levels of M1-type macrophage markers in RAW264.7 macrophages. (B) Detection of protein expression levels and localization of CD86 and iNOS in RAW264.7 macrophages was determined using an immunofluorescence assay. Magnification, x630. (C) mRNA expression levels of M1-type markers in RAW264.7 macrophages were analysed using reverse transcription-quantitative PCR. (D) M1-type marker protein expression levels in the supernatant of RAW264.7 macrophages were analysed using ELISA. Data are presented as the mean ± SEM (n=6). **P<0.01 vs. control group; #P<0.05, ##P<0.01 vs. AngII group. AngII, angiotensin II; IL, interleukin; iNOS, inducible nitric oxide synthase; PI, propidium iodide; TNF, tumour necrosis factor.
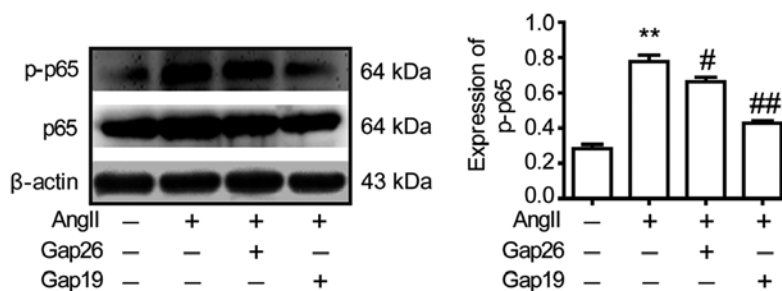

Figure 5. AngII activates the NF-κB (p65) signalling pathway through upregulating Cx43. Western blotting was performed to analyse and semi-quantify the protein expression levels of total p65 and p-p65. Data are presented as the mean ± SEM (n=6). **P<0.01 vs. control; #P<0.05, ##P<0.01 vs. AngII. AngII, angiotensin II; p, phosphorylated.

It has previously been demonstrated that gap junction channels and hemichannels composed of Cxs are found in almost all cells and tissues; however, their role in the immune response and pathological conditions has only recently been studied (33). Cx43 is one of the basic components of gap junctions and hemichannels, which are opened by changes in extracellular conditions (34). Cx43 is present in numerous types of cells, such as smooth muscle cells, resident and circulating leukocytes (neutrophils and dendritic cells), lymphocytes, activated macrophages, mast cells and some endothelial cells (35).

Cx43 deficiency has been reported to increase mortality in a mouse model of bacterial peritonitis, and Cx43 is reportedly upregulated in macrophages following LPS treatment (36). Shen et al (36) suggested that Cx43 expression in macrophages was associated with macrophage migration, an important immune process in the host defence against infection. In addition, Nie et al (37) demonstrated that the expression levels of Cx43 in mouse dendritic cells were significantly increased following AngII treatment. Immunofluorescence staining of Cx43, CD86 and iNOS was used to investigate the effect of

AngII on macrophage polarization and it was discovered that Cx43 was expressed in RAW264.7 macrophages. Moreover, some of these results are consistent with the Shen et al (36) study. In addition, AngII treatment increased the expression levels of CD86, iNOS and Cx43, which indicated that Cx43 may be involved in the M1-type macrophage polarization process.

In the present study, the pre-treatment of macrophages with two specific blockers of Cx43, Gap26 (a gap junction blocker) and Gap19 (a specific hemichannel blocker), was observed to decrease the mRNA and protein expression levels of M1-type macrophage polarization markers; Gap19 was more effective compared with Gap26 in suppressing the M1-type polarization index. Cxs are integral membrane proteins, and a hemichannel is formed by six Cx monomers in the plasma membrane. Hemichannel interactions facilitate the exchange of ions and small molecules, which forms the basis of gap junction intercellular communication (38). Within an in vitro model of ischaemia/reperfusion (I/R) injury, Yin et al (34) reported that the concentration of anti-inflammatory cytokines in the oxygen-glucose deprivation/reperfusion group is significantly decreased, while the concentration of anti-inflammatory cytokines increases after Gap19 treatment; however, Gap26 treatment only increased IL-10 concentration. These results are consistent with the results obtained in this study. Thus, it was hypothesized that the hemichannel may serve a more significant role in the polarization process compared with gap junction channels; however, the exact mechanism that led to these results remains relatively unclear and requires further investigations. Huang et al (39) studied the therapeutic effects of two specific Cx43 inhibitors, Gap26 and Gap27, on the development of allergic airway disease in mice. These studies suggest that Gap26 also has protective effects against other diseases. Hawat et al (40) demonstrated that the Cx43 inhibitor Gap26 protected intact hearts from I/R injury, either before or after ischaemia. The results from this study are consistent with the results reported in the aforementioned studies.

In a previous study, immunofluorescence staining of pan-macrophages (CD68), pro-inflammatory M1 macrophages (CD86) and remodelling M2 macrophages (CD206) was used to investigate the effect of chitosan/hyaluronic acid (CS/HA) hydrogel on macrophage polarization; the number of M1 pro-inflammatory cells was similar among the three groups (the control group, Fibrin gel group and CS/HA hydrogel group); however, the CS/HA hydrogel markedly increased the number of M2-type cells (41). The present results are consistent with this previous study (41), suggesting that CD86 and CD206 are expressed in macrophages. Another study investigated the effect of plumbagin (PL) on iNOS expression in LPS-activated BV-2 microglial cells; it was discovered that in the absence of LPS stimulation, iNOS was not expressed in resting cells and PL-treated cells, whereas in the presence of LPS, iNOS expression was detected; however, this effect was attenuated in LPS and PL co-treated cells (42). Thus, it was concluded that AngII may induce the polarization of RAW264.7 macrophages to the M1-type through upregulating Cx43.

It has been reported that the activation of NF-κB (p65) signalling is dependent on Cx43 (32). The phosphorylation of p65 is an essential step in the NF-κB signalling cascade;

and transfection with small interfering RNA targeting Cx43 or treatment with a NF-κB (p65) inhibitor was found to significantly reduce mechanically induced inflammation (32). Chen et al (32) reported that the Cx43 hemichannel served an important role in the development of ossification of the posterior longitudinal ligament through mechanical signal transduction, which subsequently activated the NF-κB (p65) signalling pathway in ligament fibroblasts and the inflammatory response in longitudinal ligament ossification cells. In the present study, the possible relationship between Cx43 and the NF-κB (p65) signalling pathway was investigated in the cellular model, as both Cx43 and NF-κB (p65) signalling pathways were activated by AngII. Alonso et al (43) discovered that AngII could increase the expression levels of Cx43 in A7r5 cells through activating the NF-κB pathway. In addition, another study revealed that oxidized low-density lipoprotein could increase the expression of Cx43 in rat thoracic aortic vascular smooth muscle cells, and these effects were prevented following pre-treatment with BAY117082 (44). Based on these studies, it was hypothesized that AngII activation may upregulate Cx43 expression through the NF-κB (p65) signalling pathway. In the present study, it was further observed that when RAW264.7 macrophages were pre-treated with Gap26 and Gap19, the protein expression levels of p-p65 were decreased in macrophages, particularly following the pre-treatment with Gap19. These results indicated that AngII activation may activate the NF-κB (p65) signalling pathway through upregulating Cx43 expression. In conclusion, the present study discovered that AngII may activate the polarization of RAW264.7 macrophages to the M1-type through the Cx43/NF-κB (p65) signalling pathway.

Availability of data and materials

The datasets used and/or analysed during the current study are available from the corresponding author on reasonable request.

Authors' contributions

LWu, KC, LWa and KM performed study design. LWu, KC, JiX and JuX performed data collection and statistical analysis. LZ, XL, LL and JS performed data interpretation. LWu, KC, LWa and KM performed manuscript preparation. LWu, KC, JiX and LZ performed literature search. XL, LL, LWa and JS collected funds. All authors read and approved the final manuscript.

Ethics approval and consent to participate

Not applicable.

Patient consent for publication

Not applicable.

Competing interests

The authors declare that they have no competing interests.

References

1. Wang Y, Xie Y, Zhang A, Wang M, Fang Z and Zhang J: Exosomes: An emerging factor in atherosclerosis. Biomed Pharmacother 115: 108951, 2019.
2. Zhou M, Ren P, Zhang Y, Li S, Li M, Li P, Shang J, Liu W and Liu H: Shen-Yuan-Dan capsule attenuates atherosclerosis and foam cell formation by enhancing autophagy and inhibiting the PI3K/Akt/mTORC1 signaling pathway. Front Pharmacol 10: 603, 2019.
3. Moore KJ, Sheedy FJ and Fisher EA: Macrophages in atherosclerosis: A dynamic balance. Nat Rev Immunol 13: 709-721, 2013.
4. Groh L, Keating ST, Joosten LAB, Netea MG and Riksen NP: Monocyte and macrophage immunometabolism in atherosclerosis. Semin Immunopathol 40: 203-214, 2018.
5. Mohammadi S, Saghaeian-Jazi M, Sedighi S and Memarian A: Sodium valproate modulates immune response by alternative activation of monocyte-derived macrophages in systemic lupus erythematosus. Clin Rheumatol 37: 719-727, 2018.
6. Stöger JL, Gijbels MJ, van der Velden S, Manca M, van der Loos CM, Biessen EA, Daemen MJ, Lutgens E and de Winther MP: Distribution of macrophage polarization markers in human atherosclerosis. Atherosclerosis 225: 461-468, 2012.
7. Binesh A, Devaraj SN and Devaraj H: Expression of chemokines in macrophage polarization and downregulation of NF-κB in aorta allow macrophage polarization by diosgenin in atherosclerosis. J Biochem Mol Toxicol 34: e22422, 2020.
8. Zhou S, Lu H, Chen R, Tian Y, Jiang Y, Zhang S, Ni D, Su Z and Shao X: Angiotensin II enhances the acetylation and release of HMGB1 in RAW264.7 macrophage. Cell Biol Int 42: 1160-1169, 2018.
9. Manucha W: Mitochondria and oxidative stress participation in renal inflammatory process. Medicina (B Aires) 74: 254-258, 2014 (In Spanish).
10. Mitchell S, Vargas J and Hoffmann A: Signaling via the NF-κB system. Wiley Interdiscip Rev Syst Biol Med 8: 227-241, 2016.
11. Ding H, Zhou Y and Huang H: MiR-101a ameliorates AngII-mediated hypertensive nephropathy by blockade of TGFβ/Smad3 and NF-κB signalling in a mouse model of hypertension. Clin Exp Pharmacol Physiol 46: 246-254, 2019.
12. Willebrords J, Crespo Yanguas S, Maes M, Decrock E, Wang N, Leybaert L, Kwak BR, Green CR, Cogliati B and Vinken M: Connexins and their channels in inflammation. Crit Rev Biochem Mol Biol 51: 413-439, 2016.
13. Donahue HJ, Qu RW and Genetos DC: Joint diseases: From connexins to gap junctions. Nat Rev Rheumatol 14: 42-51, 2017.
14. Glass AM, Snyder EG and Taffet SM: Connexins and pannexins in the immune system and lymphatic organs. Cell Mol Life Sci 72: 2899-2910, 2015.
15. Jia G, Mitra AK, Cheng G, Gangahar DM and Agrawal DK: Angiotensin II and IGF-1 regulate connexin43 expression via ERK and p38 signaling pathways in vascular smooth muscle cells of coronary artery bypass conduits. J Surg Res 142: 137-142, 2007.
16. Sarieddine MZ, Scheckenbach KE, Foglia B, Maass K, Garcia I, Kwak BR and Chanson M: Connexin43 modulates neutrophil recruitment to the lung. J Cell Mol Med 13: 4560-4570, 2009.
17. Li M, Liu JT, Pang XM, Han CJ and Mao JJ: Epigallocatechin-3-gallate inhibits angiotensin II and interleukin-6-induced C-reactive protein production in macrophages. Pharmacol Rep 64: 912-918, 2012.
18. Yang LX, Liu H, Guo RW, Ye J, Wang XM, Qi F, Guo CM and Liang X: Angiotensin II induces EMMPRIN expression in THP-1 macrophages via the NF-kappaB pathway. Regul Pept 163: 88-95, 2010.
19. Desplantez T, Verma V, Leybaert L, Evans WH and Weingart R: Gap26, a connexin mimetic peptide, inhibits currents carried by connexin43 hemichannels and gap junction channels. Pharmacol Res 65: 546-552, 2012.
20. Li W, Bao G, Chen W, Qiang X, Zhu S, Wang S, He M, Ma G, Ochani M, Al-Abed Y, et al: Connexin 43 hemichannel as a novel mediator of sterile and infectious inflammatory diseases. Sci Rep 8: 166, 2018.
21. Liang S, Chen Z, Jiang G, Zhou Y, Liu Q, Su Q, Wei W, Du J and Wang H: Activation of GPER suppresses migration and angiogenesis of triple negative breast cancer via inhibition of NF-κB/IL-6 signals. Cancer Lett 386: 12-23, 2017.
22. Strickson S, Campbell DG, Emmerich CH, Knebel A, Plater L, Ritorto MS, Shpiro N and Cohen P: The anti-inflammatory drug BAY 11-7082 suppresses the MyD88-dependent signalling network by targeting the ubiquitin system. Biochem J 451: 427-437, 2013.
23. Livak KJ and Schmittgen TD: Analysis of relative gene expression data using real-time quantitative PCR and the 2(-Delta Delta C(T)) method. Methods 25: 402-408, 2001.
24. Hansson GK, Robertson AK and Söderberg-Nauclér C: Inflammation and atherosclerosis. Annu Rev Pathol 1: 297-329, 2006.
25. Shao BZ, Han BZ, Zeng YX, Su DF and Liu C: The roles of macrophage autophagy in atherosclerosis. Acta Pharmacol Sin 37: 150-156, 2016.
26. Han X, Ni J, Wu Z, Wu J, Li B, Ye X, Dai J, Chen C, Xue J, Wan R, et al: Myeloid-specific dopamine D2 receptor signaling controls inflammation in acute pancreatitis via inhibiting M1 macrophage. Br J Pharmacol: Feb 14, 2020 (Epub ahead of print).
27. Tabas I and Bornfeldt KE: Macrophage phenotype and function in different stages of atherosclerosis. Circ Res 118: 653-667, 2016.
28. Guo F, Chen XL, Wang F, Liang X, Sun YX and Wang YJ: Role of angiotensin II type 1 receptor in angiotensin II-induced cytokine production in macrophages. J Interferon Cytokine Res 31: 351-361, 2011.
29. Jiang Q, Pan D, Yang Y, Hu Y, Fang L, Shang P, Xia Y and Li D: Luteolin regulates macrophage polarization via the PI3K/Akt pathway to inhibit the apoptosis stimulated by angiotensin II. Curr Pharm Biotechnol 19: 428-437, 2018.
30. Kim KN, Ko SC, Ye BR, Kim MS, Kim J, Ko EY, Cho SH, Kim D, Heo SJ and Jung WK: 5-Bromo-2-hydroxy-4-methyl-benzaldehyde inhibited LPS-induced production of pro-inflammatory mediators through the inactivation of ERK, p38, and NF-κB pathways in RAW 264.7 macrophages. Chem Biol Interact 258: 108-114, 2016.
31. Gupta A, Niger C, Buo AM, Eidelman ER, Chen RJ and Stains JP: Connexin43 enhances the expression of osteoarthritis-associated genes in synovial fibroblasts in culture. BMC Musculoskelet Disord 15: 425, 2014.
32. Chen D, Chen Y, Li T, Shi L, Pan M and Chen D: Role of cx43-mediated NFκB signaling pathway in ossification of posterior longitudinal ligament: An in vivo and in vitro study. Spine (Phila Pa 1976) 42: E1334-E1341, 2017.
33. Legein B, Temmerman L, Biessen EA and Lutgens E: Inflammation and immune system interactions in atherosclerosis. Cell Mol Life Sci 70: 3847-3869, 2013.
34. Yin X, Feng L, Ma D, Yin P, Wang X, Hou S, Hao Y, Zhang J, Xin M and Feng J: Roles of astrocytic connexin-43, hemichannels, and gap junctions in oxygen-glucose deprivation/reperfusion injury induced neuroinflammation and the possible regulatory mechanisms of salvianolic acid B and carbenoxolone. J Neuroinflammation 15: 97, 2018.
35. Pfenniger A, Chanson M and Kwak BR: Connexins in atherosclerosis. Biochim Biophys Acta 1828: 157-166, 2013.
36. Shen C, Chen JH, Lee Y, Hassan MM, Kim SJ, Choi EY, Hong ST, Park BH and Park JH: mTOR- and SGK-mediated connexin 43 expression participates in lipopolysaccharide-stimulated macrophage migration through the iNOS/Src/FAK axis. J Immunol 201: 2986-2997, 2018.
37. Nie W, Yan H, Li S, Zhu W, Fan F and Zhu J: Angiotensin II promotes atherogenesis through upregulating the expression of connexin 43 in dendritic cells. Cell Mol Biol (Noisy-le-grand) 61: 96-101, 2015.
38. Kim Y, Davidson JO, Green CR, Nicholson LFB, O'Carroll SJ and Zhang J: Connexins and pannexins in cerebral ischemia. Biochim Biophys Acta Biomembr 1860: 224-236, 2018.
39. Huang JQ, Chen XY, Huang F, Fan JM, Shi XW and Ju YK: Effects of connexin 43 inhibition in an ovalbumin-induced mouse model of asthma. Iran J Allergy Asthma Immunol 17: 29-38, 2018.
40. Hawat G, Benderdour M, Rousseau G and Baroudi G: Connexin 43 mimetic peptide Gap26 confers protection to intact heart against myocardial ischemia injury. Pflugers Arch 460: 583-592, 2010.

41. Deng Y, Ren J, Chen G, Li G, Wu X, Wang G, Gu G and Li J: Injectable in situ cross-linking chitosan-hyaluronic acid based hydrogels for abdominal tissue regeneration. Sci Rep 7: 2699, 2017.

42. Messeha SS, Zarmouh NO, Mendonca P, Kolta MG and Soliman KFA: The attenuating effects of plumbagin on pro-inflammatory cytokine expression in LPS-activated BV-2 microglial cells. J Neuroimmunol 313: 129-137, 2017.

43. Alonso F, Krattinger N, Mazzolai L, Simon A, Waeber G, Meda P and Haefliger JA: An angiotensin II- and NF-kappaB-dependent mechanism increases connexin 43 in murine arteries targeted by renin-dependent hypertension. Cardiovasc Res 87: 166-176, 2010.

44. Wang M, Wu Y, Yu Y, Fu Y, Yan H, Wang X, Li T, Peng W and Luo D: Rutaecarpine prevented ox-LDL-induced VSMCs dysfunction through inhibiting overexpression of connexin 43. Eur J Pharmacol 853: 84-92, 2019.